Portable Automatic Microring Resonator System Using a Subwavelength Grating Metamaterial Waveguide for High-Sensitivity Real-Time Optical-Biosensing Applications

Varun Soni [†], Ching-Wen Chang [†,*], Xiaochuan Xu, Chao Wang, Hai Yan, Michael D'Agati, Li-Wei Tu, Quark Yungsung Chen, Huiping Tian, Ray T. Chen[*]

***Abstract*—The slow light sensor techniques have been applied to bio-related detection in the past decades. However, similar testing-systems are too large to carry to a remote area for diagnosis or point-of-care testing. This study demonstrated a fully automatic portable biosensing system based on the microring resonator. An optical-fiber array mounted on a controller based micro-positioning system, which can be interfaced with MATLAB to locate a tentative position for light source and waveguide coupling alignment. Chip adapter and microfluidic channel could be packaged as a product such that it is cheap to be manufactured and can be disposed of after every test conducted. Thus, the platform can be more easily operated via an ordinary user without expertise in photonics. It is designed based on conventional optical communication wavelength range. The C-band superluminescent-light-emitting-diode light source couples in/out the microring sensor to obtain quasi-TE mode by grating coupler techniques. For keeping a stable chemical binding reaction, the cost-effective microfluidic pump was developed to offer a specific flow rate of 20 µL/min by using a servo-motor, an Arduino board, and a motor driver. The subwavelength grating metamaterial ring resonator shows highly sensitive sensing performance via surface index changes due to biomarker adhered on the sensor. The real-time peak-shift monitoring shows 10 µg/mL streptavidin detection of limit based on the biotin-streptavidin binding reaction. Through the different specific receptors immobilized on the sensor surface, the system can be utilized on the open applications such as heavy metal detection, gas sensing, virus examination, and cancer marker diagnosis.**

***Index Terms*—Subwavelength grating metamaterial, Microring resonator, Optical biosensor, Microfluidic channel**

I. Introduction

As human life span gets longer, the healthcare industry has faced ever growing pressure in many fronts to accommodate the higher needs of a larger aged population. Modern technology, especially those of fast screening and early diagnosis, has been widely embraced by the care providing systems at a time when cost effectiveness and viability become one of their major concerns. In clinical encounter, the impacts of diseases on the human body vary from case to case. In terms of time span, it may take hours or days to incubate for the hemorrhagic fever virus, coronavirus or from several months to several years for tumors and cancers to develop. Therefore, abilities to reliably identify and to quantitatively characterize the core issues have become a critical focus in development of biosensors. Following Drs. Clark and Lyon's invention of the

This work was supported by NASA STTR program (80NSSC18P2009), the US Department of Energy SBIR program (DE SC-0013178), AFOSR MURI program (FA9550-08-1-0394), National Science Foundation (Contract No. NSF-1711824), National Cancer Institute/National Institutes of Health (NCI/NIH) (Contract #: 1R43HG009113-01A1). C. W. Chang's works is supported under Ministry of Science and Technology, Taiwan, ROC (105-2911-I-110-512, 106-2911-I-110-503, 108-2320-B-110 -004). C. Wang's work is supported under National Natural Science Foundation of China (No.61634006, No.61372038), and Fund of Joint Laboratory for Undersea Optical Networks, China Scholarship Council (201806470008).

Varun Soni[†] is with the Department of Mechanical Engineering, The University of Texas at Austin, Austin, TX 78758, USA.

Ching-Wen Chang[†,*] is with Department of Electrical and Computer Engineering, The University of Texas at Austin, Austin, TX 78758, USA; Research Center for Applied Sciences, Academia Sinica, Taipei, Taiwan 11529, ROC; and Department of Physics and Center of Crystal Research, National Sun Yat-sen University, Kaohsiung, Taiwan 80424, ROC. (e-mail: cwchang@g-mail.nsysu.edu.tw).

Xiaochuan Xu is with Department of Electrical and Computer Engineering, The University of Texas at Austin, Austin, TX 78758, USA; Omega Optics Inc., 8500 Shoal Creek Blvd., Austin, TX, 78759, USA; and State Key Laboratory on Tunable Laser Technology, Harbin Institute of Technology, Shenzhen, Guangdong 518055, China.

Chao Wang is with Department of Electrical and Computer Engineering, The University of Texas at Austin, Austin, TX 78758, USA; and State Key Laboratory of Information Photonics and Optical Communications, Beijing University of Posts and Telecommunications, Beijing 100876, China.

Hai Yan is with Department of Electrical and Computer Engineering, The University of Texas at Austin, Austin, TX 78758, USA.

Michael D'Agati is with Department of Electrical and Computer Engineering, The University of Texas at Austin, Austin, TX 78758, USA.

Li-Wei Tu is with Department of Physics and Center of Crystal Research, National Sun Yat-sen University, Kaohsiung, Taiwan 80424, ROC; and Department of Medical Laboratory Science and Biotechnology, Kaohsiung Medical University, Kaohsiung, Taiwan 80708, ROC.

Quark Yungsung Chen is with Department of Physics and Center of Crystal Research, National Sun Yat-sen University, Kaohsiung, Taiwan 80424, ROC.

Huiping Tian is with State Key Laboratory of Information Photonics and Optical Communications, Beijing University of Posts and Telecommunications, Beijing 100876, China.

Ray T. Chen[*] is with Department of Electrical and Computer Engineering, The University of Texas at Austin, Austin, TX 78758, USA. He is also with Omega Optics Inc., 8500 Shoal Creek Blvd., Austin, TX, 78759, USA. (e-mail: chen@ece.utexas.edu).

[†]Contributed equally to the research. Joint first authors.

[*]Corresponding author.

first biosensor based on the concept of glucose enzyme electrode in 1962 [1], Yellow Spring Instrument Company (YSI) had been actively engaged in advancing the technology [2]. Hence it is proper to say that the first-generation biosensors started with the blood glucose enzyme electrode approach [3], though, since then, the blood glucose testing techniques have been significantly refined, aided both by fast-progressing automation and sensing technologies. Now it needs less than one minute to complete a whole test for what would take days to do the same, making live-tracking and controls of diabetes possible. By 1980, biosensors have evolved to include use of antibodies or receptor proteins as the detecting elements and molecular recognitions have since become a common practice. There are many types of signal detection methods in this regard and the adoption depends on the nature of the involved targets to detect. Currently, the biosensor developments are more focused on high performance "lab-on-a-chip" approach that offers high sensitivity, high selectivity, and high specificity so that rapid real-time tests can be conducted with more user-friendly human-machine interfaces to deal with complex measurements. However, while recent advances in the field have been significant, the challenges to promoting the "lab-on-a-chip" technology remain high in various fronts.

Silicon photonics continues to enjoy wide acceptance because of its compatibility with complementary metal-oxide-semiconductor (CMOS) fabrication processes for highly integrated photonic chips at low cost and light travels faster than electrons and thus can provide enhanced communication passages at higher speeds. Starting with long-haul communication systems, applications range from optical routers and signal processors to biosensing. Recently, interests in silicon photonics based biosensing has been on the rise, owing to, among other things, lower cost, real-time, and label-free detections of reachable high sensitivity and throughput [4]–[6]. Many such devices, such as 1-dimensional and 2-dimensional photonics crystal micro-cavities for biosensing [7]–[10], silicon nanowires [11], surface-plasmon devices [12]–[14], microring resonators [15]–[17], and microrings based on subwavelength grating structure [18], [19] have been demonstrated and built into instruments. Pharmacia Biosensor AB (now Biacore AB since 1996) produced the first commercial surface plasmon resonance (SPR) based system in 1990 [20], [21]. Since then, Biacore AB has offered many other kinds of systems and provided those of highest sensitivities reaching the limit of detection at 1 pM, while BioNavis [22], Bio-Rad [23], ForteBio [24], and Carterra [25] have also developed similar SPR sensing products. In addition to those mentioned above, enzyme linked immunosorbent assay (ELISA) [26], electrochemical sensor [27], [28], micro-electrode immunoassay [29], and high performance liquid chromatography [30] have been already commercially used universally. The portable system reported herein has significant advantages over its traditional desktop counterparts due to the smaller sizes, faster real-time readouts, higher sensitivities, and matches with the optical telecommunication bands.

One of the issues with planar waveguide sensors and surface plasmon resonance sensors is in the difficulty of being made compact enough that is suitable for a lab on the chip. In addition, photonic crystal microcavity biosensor has lower sensitivity than those of microring resonators [31]. Silicon-on-insulator (SOI) microring resonators have demonstrated greater potential among all other sensors because of their compact size and high sensitivity [32]–[38]. The bulk sensitivity of strip silicon microring resonator was found to be 57 nm/RIU [38]. By decreasing the waveguide thickness to 90 nm, the sensitivity were improved to 100 nm/RIU [39] nm due to the increase in overlapping of electric field with the analyte. Many kinds of innovative waveguide structures, such as slot waveguide [40]–[42], subwavelength grating metamaterial (SGM) [18], [43]–[47] and nanoporous materials [48]–[50], have been investigated and all showed improved sensitivity for the ring resonators. Couplings of light between an optical fiber and a planar waveguide based on the SGM waveguide concept have been previously proposed [51] and later demonstrated [52] in 2010. The macroscopic optical properties of SGM can be readily tailored by controlling the geometry of the artificial structures [53], [54]. As an extension to this, many research groups have proposed SGM waveguide for biosensing and chemical sensing [18], [46], [53], [55], [56]. Gonzalo Wangüemert-Pérez *et al.* provided the first theoretical analysis of SGM waveguide [53]. In this work, a microring resonator based on SGM structure [18] has been demonstrated as an automated portable bio-sensing system of superior sensitivity. By tuning the duty cycles of the SGM structure to adjust the equivalent effective index of the microring waveguide, the free spectral range (FSR) and bulk sensitivity can be greatly increased. According to effective medium theory, it can also be considered as a continuous waveguide made of a uniform material [19]. Several experimental results demonstrated that the bulk sensitivity of SWG microring resonator could be more than 400 nm/RIU [18], [44], [45], [56]. By decreasing the asymmetric refractive index distribution via undercut pedestal SGM design, the bulk sensitivity has been improved to 545 nm/RIU [19]. Integrated hundreds of microring resonator devices on a single chip provides competitive throughput on multiple sensing channels approaches [34]. According to the above advantages, microring resonator device has a significant potential on the biosensing applications. In addition to biosensor chip design, another important aspect is to achieve continuous flow of analyte on chip surface. Integration of microfluidics with photonic sensors results in reduction in sample-consumption, shorter analysis time, portability, and achieving integrated biosensors [57]. A polydimethylsiloxane (PDMS) based microfluidic channel fabricated following laser cutting and surface oxygen plasma modification has been used to allow biomolecules flow on silicon chips in a controlled manner. User-friendly system-computer interface has been implemented with MATLAB (MathWork, Natick, Massachusetts, USA) to control the coupling position of optical fibers, motion of the microfluidic stage, and data collection of the optical spectra, all in an automated manner. This would thus bypass the lengthy efforts of laboratory tests that require much professional expertise on the optical path alignment and spectra collection steps. The achieved rapid real-time tests offer excellent capacities of a quickly updated database for clinical and scientific research needs.

II. Experimental Setup

The demonstrated system includes 8 parts composed of (1) a cost-efficient microfluidic pump to drive a force for bio-samples injection, (2) a micro-positioning system to provide the fiber array move to the particular sample position for light coupling in/out the waveguide, (3) a chip holder/ adapter/mounting stage, (4) a broadband superluminescent light-emitting diode (SLED) covering 1530-1570 nm as the light source, (5) an optical spectrum analyzer to measure the transmission spectrum of microring resonator biosensor, (6) a 4 channel single mode optical-fiber array (7) a power meter to obtain the fine alignment of light coupling in/out the waveguide, and (8) a Si photonics biosensor chip. The main mechanical operation platform is assembled into a square area of 20.32 cm×20.32 cm (8 inch×8 inch) (Fig. 1 (a)). Also included in the total system are the associated system-computer electric circuit, cables, fibers, and power supplies, all contained in a 35.36 cm×35.56 cm×22.86 cm (14 inch×14 inch×9 inch) box (Fig. 1 (b)) which can be further reduced if the cables and fibers length are properly adjusted.

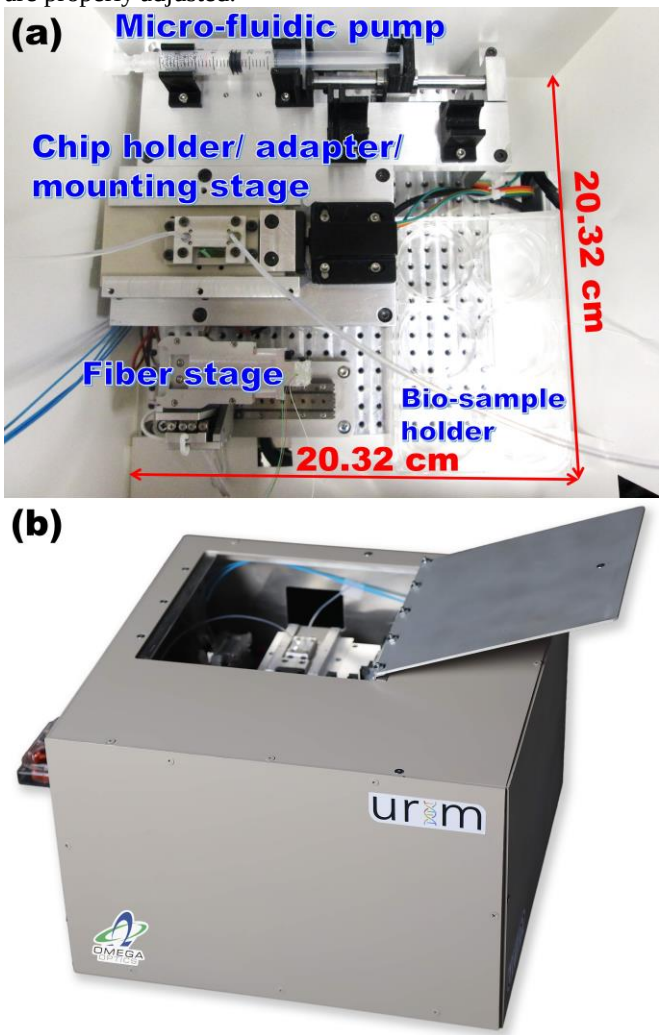

Fig. 1 (a) The main operation platform which includes a microfluidic pump, a chip holder/ adapter/ mounting stage, a fiber holder, and bio-sample holder. (b) The outward appearance of the system. All devices are assembled in a 35.36 cm×35.56 cm×22.86 cm box.

A. Cost-efficient microfluidic pump layout

Microfluidic operation is an essential part of the lab-on-chip sensing system. It can provide a steady reaction cavity of stable liquid flow rate to a reduced bio-sample and reagent volumes through which enhanced detection efficiency can be achieved in miniaturizing traditional bio-testing onto a single chip.

In this section, the cost-effective microfluidic pumping design is described. It consists of a servo motor, an Arduino Uno microcontroller, and a motor driver L298D. The flow rate of biomolecules falls in the range of Q = 20 µL/min. The relationship between microfluidic flow rate and rotating rate of the servo motor can be calculated according to the following equation:

$$N = 4Q/(\pi d^2 p), \quad (1)$$

where N is revolutions per minute of servo motor, Q is flow rate in L/min, d is diameter of syringe in mm, and p is pitch of lead screw of servo motor in mm. For instance, for a syringe diameter of 8.66 mm and pitch of lead screw of 1 mm, to reach the flow rate of 20 µL/min requires an angular velocity of servo motor to be 0.34 rpm. A MATLAB program is developed to control the servo motor rotation in accordance with Eq. 1 given above.

As shown in Fig. 2, Syringe 1, which is connected to the servo motor and rotary to linear motion converter, acts as the primary source of biomolecular flow, while Syringe 2 serves as a secondary entity. When the Syringe 1 is filled, Syringe 2 comes in as a replacement. Syringe 2 also can be used to provide biomolecular flow manually, but in manual operation, it is difficult to maintain a steady flow rate.

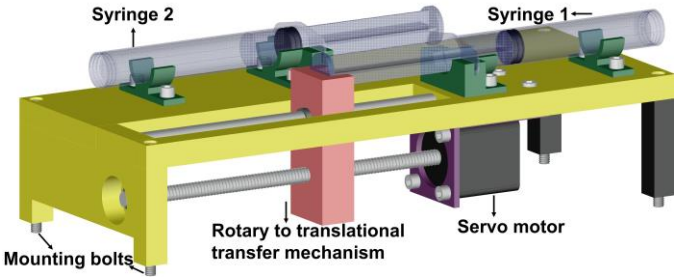

Fig. 2 The schematic design of microfluidic pump.

B. Micro-positioning system configuration

Aligning the optical fiber with a waveguide on silicon chip using grating coupler requires significant experience for photonics professionals, so it can indeed be a challenge for medical laboratory people to operate the silicon-chip system with ease for biosensing. To alleviate this situation, the optical fiber has been mounted on a microcontroller-based micro-positioning system (SmarAct GmbH), interfaced with a MATLAB program to eliminate dependency on the users to align optical fiber with waveguide on the chip. This system has a tolerance in a range of 1 µm and 4 degrees of freedom, including the x-axis, y-axis, and z-axis for linear motions and the rotation-axis (ϕ) for rotary motion. Its mechanism of motion is illustrated in Fig. 3. When the user clicks on "Chip" button of "Test Bench GUI" page in the system program, it aligns the optical fiber with the waveguide on chip. Then, the MATLAB program moves the micro-positioning system in pre-defined steps in a configurable search window to find the position that gives maximum output power. This position is fixed, and the optical power values are taken at this point. Furthermore, the

fiber and the grating coupler are coupled nicely to obtain a high coupling efficiency via the "Fine Align" button. After measurement, the user just needs to select the "Home" button to return the fiber stage to its original point. The mechanism of actions is demonstrated in the supplementary video (00:32-00:46).

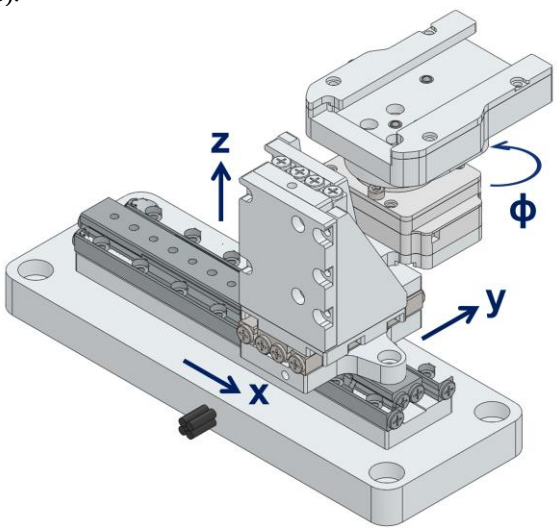

Fig. 3 The schematic design of fiber micro-positioning system.

C. Microfluidic channel, chip holder, adapter, and mounting stage

1) Microfluidic channel

A PDMS based microfluidic channel [58] was fabricated on the chip using soft lithography [59]. This technique was developed in our laboratory to allow for bio-molecular flow on silicon chips in a controlled manner. However, conventional soft lithography has its challenges to overcome when it comes to the microfluidic channel fabrications as the channel size is reduced and control of the bio-solution injection into a specific sensing area becomes difficult. To circumvent this, 3-dimensional microfluidic channels of 4 different layers are created via oxygen plasma surface modifications to provide strong permanent PDMS-PDMS binding assisted by siloxane bonding. The top-right inset of Fig. 4 (a) shows a 3-dimensional PDMS microfluidic channel with its layouts on each layer. All slots and holes of the four PDMS layers were made by laser cutting. The 1st layer is developed for specific sensing area which is an important part of the chip size reduction, the 2nd layer is designed to extend the spacing of two flow-in/out tubing, while the 3rd and 4th layers are there to fix the tubing. The parameters of oxygen plasma surface treatment, regarding the gas pressure, electric power, gas flow rate, and treatment time were optimized at ~380 mTorr, 20 W, 15 sccm, and 30 sec, respectively, for each of the four bonded layers. On completion of the oxygen plasma treatment and activation of the surfaces of the PDMS layers, the layers were taken out of the chamber and immediately aligned and bound. As shown in Fig. 4 (a), the dyed gray water was able to go through the left entry, to flow through the microfluidic channels created inside the PDMS layers, and to come out of the right exit. It means no leakage of liquid anywhere throughout the structure. More details on the PDMS microfluidic channel fabrication process are provided in the supplementary material: Section 1.

2) Chip holder

The chip holder is shown in Fig. 4 (a) yellow part. A slot in chip holder with tolerances of ±10 μm is used to keep the chip in place. On top of the holder it sits an aluminum cap to sandwich the PDMS based microfluidic channel. Polyethylene tubing (BD Intramedic™ PE Tubing, PE 50) of 0.58 mm inner diameter has been used to inject biomolecules into the microfluidic channels. Four alignment keys are designed for PDMS layers and an aluminum cap is arranged at the holder center.

3) Adapter

The chip holder is attached to a base plate which has the male portion of a snap-fit to connect adapter with the mounting stage, as shown in Fig. 4 (a) purple part.

4) Mounting stage

Fig. 4 (a) shows the aluminum based mounting stage designed to desired length and weight. Alignment rails with tolerances of ±10 μm are used to properly snap fit the chip adapter onto the mounting stage. The snap fit mechanism has been chosen for ease of assembly and disassembly. The schematic design of assembled chip holder, adapter, and mounting stage are is shown in Fig. 4 (b).

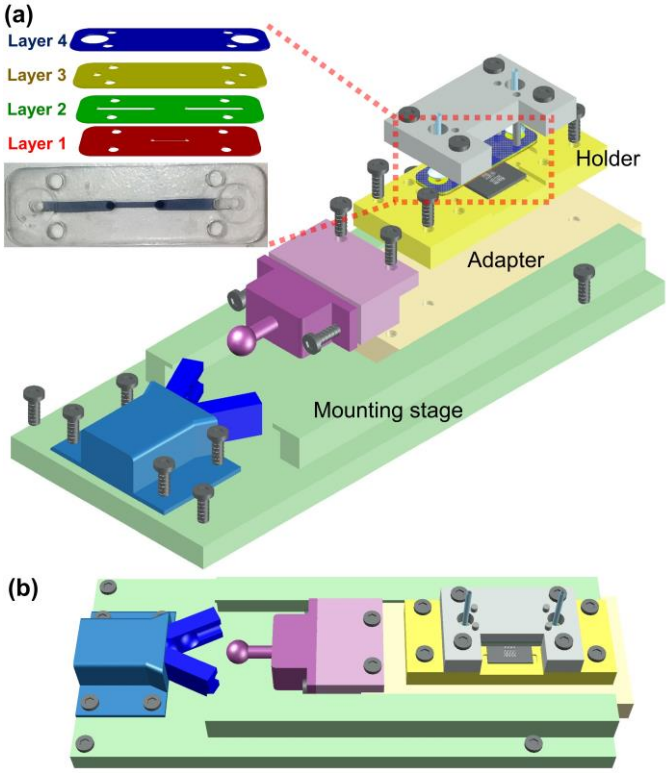

Fig. 4 (a) The exploded view of the microfluidic channel, the chip holder, the adapter, and the mounting stage. The top-left inset shows four different PDMS layers layout with thickness of 250 μm. The dyed water goes through the PDMS microfluidic channel structure which demonstrates no leaking of the channel and strong bonds of PDMS layers. (b) The top view of schematic design for the assembled chip holder, the adapter, and the mounting stage.

D. C-band light source

C-band light source (SLED, DenseLight BX9-CS5403A) has been used to couple light into the sensor waveguide through the grating coupler to obtain quasi-TE mode.

E. Optical spectrum analyzer

Light is coupled into an optical spectrum analyzer (Optoplex, OM-1C2MM353) to obtain transmission spectrum that measures wavelength shift due to surface refractive index change.

F. Optical fiber array

A 4-channel optical fiber array (PLC Connections) made to the C-band range has been used.

G. MATLAB GUI program

The original source code is written by Shon Schmidt, Jonas Flueckiger, and WenXuan Wu belong to Maple Leaf Photonics company. The micro-positioning system "Home" and "Chip" positions are defined via code modification. The control panel of the cost-efficient microfluidic pump is added in this research.

H. Optical power meter

The optical power meter (Newport 1830-R) and power detector (Newport 818-IR/DB) are utilized to check the fiber and waveguide fine alignment.

I. Silicon bio-sensing chip

The surface sensitivity S_s can be defined as below,

$$S_s = \frac{\Delta\lambda}{\Delta t} = \frac{\lambda}{n_g}\left(\frac{\partial n_{eff}}{\partial t}\right), \quad (2)$$

where $\Delta\lambda$ is the resonance wavelength shift, Δt is the change of surface layer thickness, n_{eff} is the effective refractive index of the waveguide mode, and n_g is the group index. According to H. Yan *et al.* simulation and experimental results, the large mode overlapping factor provides the 4-6 times higher $\frac{\partial n_{eff}}{\partial t}$ in the SGM microring resonator than the regular strip microring resonator [18]. That means the SGM microring resonator has superior surface sensitivity and better sensing capability over regular strip microring resonator. Fig. S3 shows experimental surface sensitivity comparison of the SGM microring resonator and the regular strip microring resonator.

The SGM microring resonator biosensors are fabricated on SOI chips with 10 nm SiO_2 hard mask layer and 220 nm single crystal Si device layer. The optimized parameters of device structure are simulated by 3-dimensional finite-difference time-domain (FDTD) method [18]. The SGM microring resonators with diameter of the microring R = 10 μm, width of waveguide core w = 520 nm, length of silicon pillar l = 200 nm, gap between microring and bus waveguide g = 50 nm, thickness of waveguide core h = 220 nm, and grating period Λ = 250 nm are designed, as shown in Fig. 5. The chip size of 1 cm by 1 cm included 8 SGM microring resonator devices. The estimated quality factor in deionized water is $Q \sim \frac{\lambda_{resonance}}{\Delta\lambda_{3dB}} \sim 2180$ at 1548.81 nm. More details of the chip fabrication are given as a part of the supplementary materials: Section 3. It has 423 nm/RIU bulk sensitivity shown in Fig. S4. The limit of detection also can be estimated ~4.2×10^{-4} RIU with 60 pm noise level.

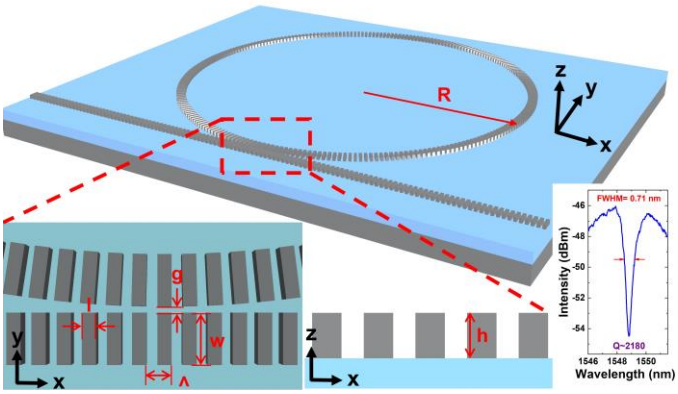

Fig. 5 The schematic of SGM waveguide microring resonator, where R is the diameter of the microring, Λ is the subwavelength grating period, h is the thickness of waveguide core, w is the width of waveguide core, l is the length of silicon pillar, and g is the gap between microring and bus waveguide. The right-bottom inset shows transmission spectrum of the fabricated SGM microring.

III. Demonstration of Biosensing

APTES ((3-Aminopropyl)-triethoxysilane) usually serves as a bridge between the semiconductor and biomolecules for which it provides an amine groups (-NH_2) on the silicon dioxide layer for molecular binding of proteins. At first, the SGM microring surface was modified by a hydroxyl group (-OH) through the piranha treatment for 1 hour (Fig. 6 (a)). Then, the SGM microring chip was soaked in a 10% diluted-APTES in pure toluene for 1 hour to form strong silanols (Si-O-H) bonding on the SGM microring surface via reactions between the methoxyl (-CH_3) and hydroxyl (-OH) radical groups (Fig. 6 (b)). The unbound APTES can be removed by thoroughly rinsing the chip with toluene and methanol. To enhance stability of the bounded molecules, the chip was baked at 110 °C for 1 hour under ambient condition. Afterwards, the 10^{-2} M EZ-LinkTM Sulfo-NHS-Biotin (Thermo ScientificTM) receptor of streptavidin was flown into the ring resonator device on the chip at a pumping speed of 20 μL/min for 1 hour (Fig. 6 (c)). Finally, the biotin receptor is expected to catch the streptavidin molecules as a consequence of their specific binding relation (Fig. 6 (d)).

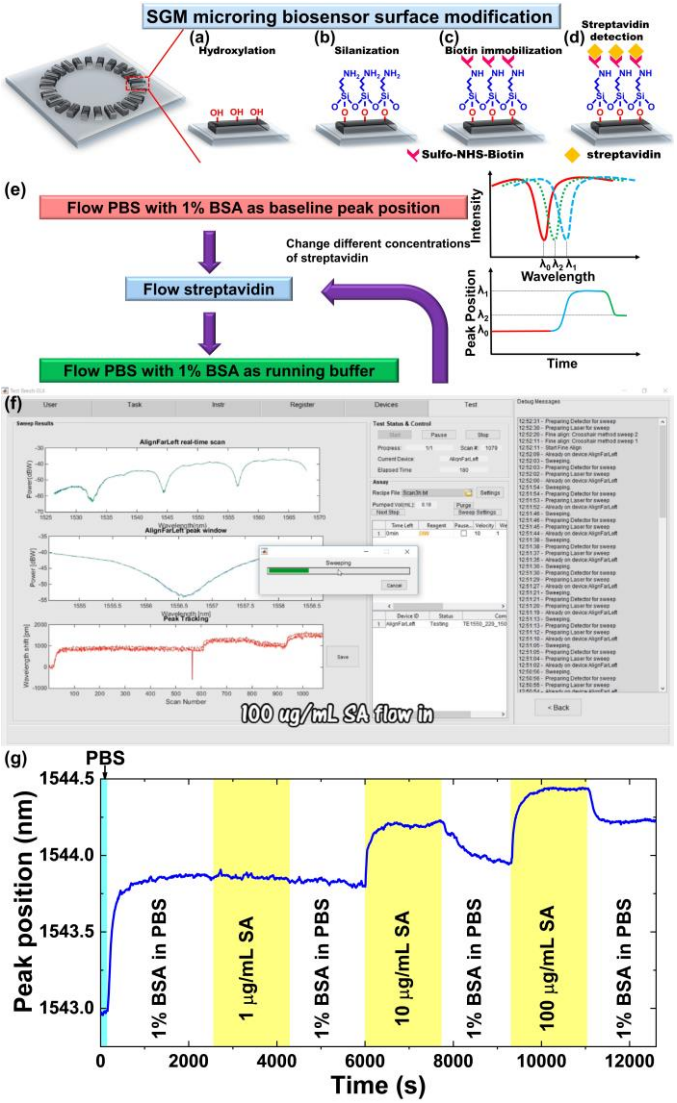

Fig. 6 The procedure of surface modification and detection of SGM microring biosensor: (a) Hydroxylation, (b) Silanization, (c) Biotin immobilization, and (d) streptavidin detection. (e) The low concentration detection flowchart and the schematic sensing results. (f) The graphical user interface for real-time biomolecules detection. (g) The real-time relative resonance peak monitored of streptavidin detection.

A phosphate-buffered saline (PBS) with 1 % bovine serum albumin (BSA) was injected into the SGM microring sensing area to measure the baseline reference resonance peak position before streptavidin detection testing [19]. As BSA can block vacancies between the APTES molecules, it is also used as a running buffer to rinse the unbound streptavidin for 30 minutes before changing concentration of the streptavidin (SA, Sigma-Aldrich) target molecular sensing. The streptavidin was prepared into different concentrations of 0.1 ng/mL, 1 ng/mL, 10 ng/mL, 100 ng/mL, 1 μg/mL, 10 μg/mL, and 100 μg/mL from the running buffer of 1 % BSA in PBS aimed for the demonstrations of a portable, highly sensitive, automated real-time optical-biosensing system. To verify the functional and device sensitivities, the streptavidin solutions were introduced sequentially over 30 minutes for each concentration. A flowchart for such tests is shown in Fig. 6 (e). The top-right inset shows a resonant peak shift due to a refractive index change induced by surface-attached biomaterials. The original peak position λ_0 (red line) will red shift to λ_1 (blue line) during the streptavidin flow. As the unbound streptavidin is removed by 1% BSA/PBS running buffer, the resonance peak would undergo a blue shift to λ_2 (green line) because of the decrease of refractive index arising from the materials incurred at surface, thus successfully demonstrating a real-time detection system. An analysis of such biomolecular detection as a case in point is given in Fig. 6 (f) for a real-time monitor based on the relative resonance peak shifts of the SWG microring sensor. As shown with label in Fig. 6 (g), the clear response to a low concentration of 10 μg/mL is remarkable. A dynamic real-time demonstration is provided as a supplementary video (00:58-1:32).

IV. Discussion, Improvement and Further Applications

A. The repeatability of the chip fabrications

For certifying repeatability of chip performance, two chips are fabricated under the same process parameters but not in the same batch. To compare bulk refractive index sensitivity of six same structure devices on the two chips, different concentrations of glycerol solution (0 %, 2.5 %, 5 %, 10 %, 20 %, and 40 %) were prepared and infused onto the SGM microring sensing area through microfluidic channels. The flow rate and time of each diluted glycerol solution are 50 μL/min and 8 min for 30 data points. Fig. 7 (a) shows the monitored resonance peak shift of transmission spectra for each devices on the two chips. The defination of bulk sensitivity can be written as,

$$S=\frac{\Delta\lambda}{\Delta n}, \quad (3)$$

where S is the bulk sensitivity, $\Delta\lambda$ the resonance shift, and Δn the refractive index change. Accordance with the real-time monitoring of different glycerol concentrations, the relationship of resonance peak shifts versus refractive index change is shown in Fig. 7 (b). A linear function fits well with a regression correlation coefficient r^2 = 0.9999 for all devices. The bulk sensitivity of Chip 1 for ~310 nm/RIU and Chip 2 for ~350 nm/RIU with the standard deviation as 1.7 nm/RIU and 1.5 nm/RIU, respectively. It indicated that the measurement error is lower than 1% in the same chip and the uniformity of the devices is good. However, the standard deviation of all six devices is 22.7 nm/RIU that may come from fabrication issue due to on-campus processes facilities instability.

Fig. 7 (c) shows the real-time relative resonance peak monitored of streptavidin detection. Following the procedure of surface modification and streptavidin detection of SGM microring biosensor steps in section 3, resonance peak positions of two chips were stable with the introduction of 1μg/mL streptavidin in diluted 1% BSA/PBS running buffer without obvious peak shift. A low limit concentration of 10 μg/mL (~167 nM) was detected by Chip 1. It was then noticed that the resonance peak shift of both chips is around 0.4 nm±0.02 nm for 100 μg/mL (~1.67 μM) streptavidin detection. That means SGM microring could be applied to the concentration estimation by resonance peak shift and the results could be repeatable. The streptavidin detection limitation, which considered biomolecule interaction is caused by 0.01 nm resolution spectra analyzer and the environment or manmade factors.

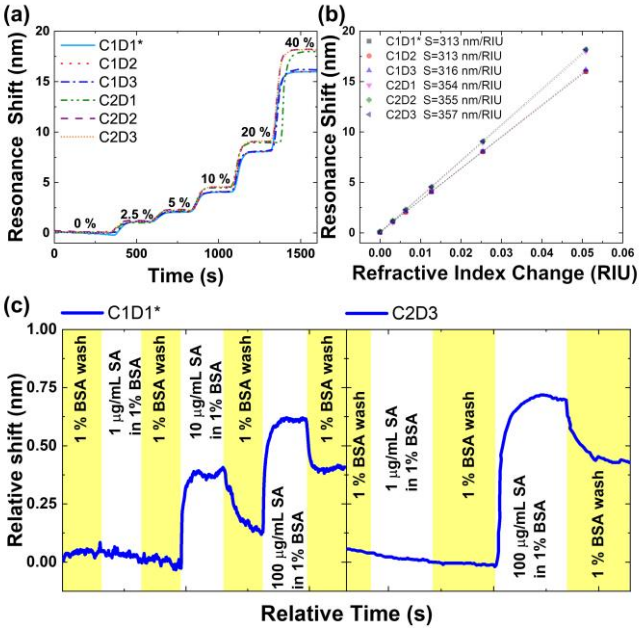

Fig. 7 (a) The resonance peak shifts of transmission spectra were monitored during the bulk refractive index change. (b) The resonance shift versus refractive index change extracted by the linear regression. The bulk sensitivities of six devices were calculated from each slope. (c) The real-time relative resonance peak monitored of streptavidin detection. (C: Chip; D: Device; *The demonstration device in the video.)

B. The optical alignment processes

All the components critical to the performance and endurance of the system have been machined to the tolerances of ±1 μm by lapping. For the fiber position calibration, the micro-positioning is accomplished by a MATLAB-based GUI to move to a tentative position on the chip for the first waveguide where a peak power is observed. The x, y, z, and θ coordinates of this position are then saved for this first waveguide. This process is repeated for all the positions on the chip and their corresponding coordinates are saved in a file. It should be noted that these coordinates are different from chip to chip, hence the coordinates for that chip saved earlier must be called in again to work with the positioning. When a user presses the 'Chip' button, the micro-positioning system moves to the tentative position of the first waveguide as read from the storage. After moving to that position, it is instructed by the computer program to scan a neighboring spatial area of 10 x 10 μm^2 seeking a peak intensity. This automated spatial scanning algorithm ensures that the optical fiber guides in a maximal amount of light into the waveguide with the system performance remain unaffected by any minor environment changes, all without human intervention. This process was replicated over all the waveguides on the chip. Moreover, the fiber positions are calibrated every 10 spectra measured so that reliable light coupling can be reassured. For the current prototype development, the system testing is placed on the optical table to avoid unnecessary environmental effects such as mechanical vibrations. Future development of systems will be focused on a system more robust against external perturbations.

C. The improvement and further applications

The demonstration in this study is based on SGM microring resonator sensor and its surface detection limit of streptavidin is 10 μg/mL (~167 nM). In fact, considering the asymmetric index distribution along the vertical direction, the pedestal SGM structures were proposed and fabricated in our group previously. The bulk sensitivity and surface sensitivity are improved by 28.8% and 1000 times by etching the undercut SiO_2 [19]. Although the demonstration was at a low concentration of streptavidin 10 μg/mL (~167 nM) under the portable optical spectrum analyzer with 0.15 nm resolution, the pedestal SGM could replace the regular SGM microring sensors and provide the streptavidin 0.1 ng/mL (~1.67 pM) limit of detection. The multiple channels SGM microring sensors could be integrated into a larger scale chip with one mask lithography process by exploiting CMOS microelectronics fabrication capability, which is a very competitive method in sensing area applications.

Based on the successful streptavidin sensing, this portable system can be applied to detect a variety of tumor markers in developing simple "lab-on-a-chip" that is low-cost and easy to use for rapid, high throughput cancer antigen sensing. The system weight (~10 kg) is also sensible for carriage that improves mobile flexibility. This would thus bypass lengthy laboratory tests that require much more professional expertise. In view of above mentioned reasons, it has a considerable potential to provide a quickly updated database to help clinical decisions or scientific research in the future. Moreover, it is an open system that can be applied in gas sensing, heavy metal identification, air- and water-pollution sensing and so on.

V. Conclusion

A fully automated portable silicon-based optical bio-sensing system has been successfully demonstrated. It is essentially based on a subwavelength grating metamaterial microring resonator structure down to the nanoscale of 50 nm. When adequately designed, the subwavelength grating metamaterial microring sensor demonstrates unprecedented sensitivity on a myriad of biomarkers. The graphic user interface written in MATLAB for system manipulation is designed with ease of use. The real-time relative resonance peak shifts observed in streptavidin detection for regular SWG microring resonators show excellent system performance. The machining demonstrations in the article and supplementary video prove that portable fully automatic silicon-based optical biosensing system is a promising platform for the detection of any biomarker or chemical molecules by surface refractive index perturbations. A low concentration of streptavidin 10 μg/mL (~1.67 nM) was detected by regular SWG microring resonators under the portable optical spectrum analyzer with 0.15 nm resolution. A property of highly movable flexibility is designed with a weight of ~10 kg. The next step of this kind of system progress is clinic blood testing research and specific gas sensing. Researchers hope this would lead eventually to practical rapid diagnostic applications not only for early cancer detection but also for post-surgery or post-treatment follow-up by providing convenience, consistency as well as efficiency.

Appendix

Supplementary video: The portable automatic system operation and streptavidin sensing demonstration.

Supplementary material: PDMS processes, SGM microring resonators fabrication.

ACKNOWLEDGMENT

This work was supported by NASA STTR program (80NSSC18P2009), the US Department of Energy SBIR program (DE SC-0013178), AFOSR MURI program (FA9550-17-1-0071), National Cancer Institute/National Institutes of Health (NCI/NIH) (Contract #: 1R43HG009113-01A1).
C. W. Chang's works is supported under Ministry of Science and Technology, Taiwan, ROC (105-2911-I-110-512, 106-2911-I-110-503, 108-2320-B-110 -004). C. Wang's work is supported under National Natural Science Foundation of China (No.61634006, No.61372038), and Fund of Joint Laboratory for Undersea Optical Networks, China Scholarship Council (201806470008).

The idea is conceived by Xiao-chuan Xu and Ray T. Chen. The human-machine interface program is optimized by Varun Soni, under the supervision of Xiao-chuan Xu. The biochip is fabricated and tested by Ching-Wen Chang, under the supervision of Xiao-chuan Xu. The final system is assembled by Ching-Wen Chang and Varun Soni with assistance from Chao Wang. The manuscript is written and organized by Ching-Wen Chang with input from Varun Soni and Xiao-chuan Xu. The video is organized by Ching-Wen Chang. Yen Hai and Michael D'Agati worked on the previous design of microfluidic channel, stages and microfluidic pump design. Ching-Wen Chang is a postdoctoral scholar supported by Li-Wei Tu and Quark Yungsung Chen. Chao is a graduate student supported by advisor Huiping Tian. We also greatly appreciate Maple Leaf Photonics company contribution on original source code.

REFERENCES

[1] L. C.Clark andC.Lyons, "Electrode Systems for Continuous Monitoring in Cardiovascular Surgery," *Ann. N. Y. Acad. Sci.*, vol. 102, no. 1, pp. 29–45, 1962, doi: 10.1111/j.1749-6632.1962.tb13623.x.

[2] L. C.Clark, "Membrane polarographic electrode system and method with electrochemical compensation," US3539455DA, 1970.

[3] L. C.Clark andC. A.Duggan, "Implanted electroenzyme glucose sensors," *Diabetes Care*, vol. 5, no. 3, pp. 174–180, 1982, doi: 10.2337/diacare.5.3.174.

[4] M. C.Estevez, M.Alvarez, andL. M.Lechuga, "Integrated optical devices for lab-on-a-chip biosensing applications," *Laser Photonics Rev.*, vol. 6, no. 4, pp. 463–487, 2012, doi: 10.1002/lpor.201100025.

[5] V. M. N.Passaro, C.deTullio, B.Troia, M.LaNotte, G.Giannoccaro, andF.DeLeonardis, "Recent advances in integrated photonic sensors," *Sensors*, vol. 12, no. 11, pp. 15558–15598, 2012, doi: 10.3390/s121115558.

[6] F.Vollmer, L.Yang, andS.Fainman, "Label-free detection with high-Q microcavities: A review of biosensing mechanisms for integrated devices," *Nanophotonics*, vol. 1, no. 3–4, pp. 267–291, 2012, doi: 10.1515/nanoph-2012-0021.

[7] F.Liang, N.Clarke, P.Patel, M.Loncar, andQ.Quan, "Scalable photonic crystal chips for high sensitivity protein detection," *Opt. Express*, vol. 21, no. 26, p. 32306, 2013, doi: 10.1364/oe.21.032306.

[8] W. C.Lai, S.Chakravarty, Y.Zou, Y.Guo, andR. T.Chen, "Slow light enhanced sensitivity of resonance modes in photonic crystal biosensors," *Appl. Phys. Lett.*, vol. 102, no. 4, p. 04111, 2013, doi: 10.1063/1.4789857.

[9] H.Yan *et al.*, "Silicon on-chip bandpass filters for the multiplexing of high sensitivity photonic crystal microcavity biosensors," *Appl. Phys. Lett.*, vol. 106, no. 12, p. 121103, 2015, doi: 10.1063/1.4916340.

[10] Y.Zou *et al.*, "Cavity-Waveguide Coupling Engineered High Sensitivity Silicon Photonic Crystal Microcavity Biosensors With High Yield," *IEEE J. Sel. Top. Quantum Electron.*, vol. 20, no. 4, pp. 171–180, 2014, doi: 10.1109/JSTQE.2013.2291443.

[11] S.Janz *et al.*, "Photonic wire biosensor microarray chip and instrumentation with application to serotyping ofEscherichia coliisolates," *Opt. Express*, vol. 21, no. 4, p. 4623, 2013, doi: 10.1364/oe.21.004623.

[12] B.Zhang, A. W.Morales, R.Peterson, L.Tang, andJ. Y.Ye, "Label-free detection of cardiac troponin I with a photonic crystal biosensor," *Biosens. Bioelectron.*, vol. 58, no. 15, pp. 107–113, 2014, doi: 10.1016/j.bios.2014.02.057.

[13] A. A.Yanik, M.Huang, A.Artar, T. Y.Chang, andH.Altug, "Integrated nanoplasmonic-nanofluidic biosensors with targeted delivery of analytes," *Appl. Phys. Lett.*, vol. 96, no. 2, pp. 1–4, 2010, doi: 10.1063/1.3290633.

[14] J. N.Anker, W. P.Hall, O.Lyandres, N. C.Shah, J.Zhao, andR. P.VanDuyne, "Biosensing with plasmonic nanosensors," *Nat. Mater.*, vol. 7, no. June, pp. 8–10, 2008, doi: 10.1038/nmat2162.

[15] M.Iqbal *et al.*, "Label-Free Biosensor Arrays Based on Silicon Ring Resonators and High-Speed Optical Scanning Instrumentation," *IEEE J. Sel. Top. Quantum Electron.*, vol. 16, no. 3, pp. 654–661, 2010.

[16] C. Y.Chao andL. J.Guo, "Biochemical sensors based on polymer microrings with sharp asymmetrical resonance," *Appl. Phys. Lett.*, vol. 83, no. 8, pp. 1527–1529, 2003, doi: 10.1063/1.1605261.

[17] M. S.McClellan, L. L.Domier, andR. C.Bailey, "Label-free virus detection using silicon photonic microring resonators," *Biosens. Bioelectron.*, vol. 31, no. 1, pp. 388–392, 2012, doi: 10.1016/j.bios.2011.10.056.

[18] H.Yan *et al.*, "Unique surface sensing property and enhanced sensitivity in microring resonator biosensors based on subwavelength grating waveguides," *Opt. Express*, vol. 24, no. 26, p. 29724, 2016, doi: 10.1364/oe.24.029724.

[19] C. W.Chang *et al.*, "Pedestal subwavelength grating metamaterial waveguide ring resonator for ultra-sensitive label-free biosensing," *Biosens. Bioelectron.*, vol. 141, no. May, p. 111396, 2019, doi: 10.1016/j.bios.2019.111396.

[20] S.Löfås andB.Johnsson, "A novel hydrogel matrix on gold surfaces in surface plasmon resonance sensors for fast and efficient covalent immobilization of ligands," *J. Chem. Soc. Chem. Commun.*, no. 21, pp. 1526–1528, 1990, doi: 10.1039/C39900001526.

[21] S.Löfås, M.Malmqvist, I.Rönnberg, E.Stenberg, B.Liedberg, andI.Lundström, "Bioanalysis with surface plasmon resonance," *Sensors Actuators B. Chem.*, vol. 5, no. 1–4, pp. 79–84, 1991, doi: 10.1016/0925-4005(91)80224-8.

[22] N.Granqvist, A.Hanning, L.Eng, J.Tuppurainen, andT.Viitala, "Label-enhanced surface plasmon resonance: A new concept for improved performance in optical biosensor analysis," *Sensors*, vol. 13, no. 11, pp. 15348–15363, 2013, doi: 10.3390/s131115348.

[23] J. C.Varada *et al.*, "A neutralization assay for respiratory syncytial virus using a quantitative PCR-based endpoint assessment," *Virol. J.*, vol. 10, no. 1, p. 1, 2013, doi: 10.1186/1743-422X-10-195.

[24] S.Naik *et al.*, "Monitoring the kinetics of the pH-driven transition of the anthrax toxin prepore to the pore by biolayer interferometry and surface plasmon resonance," *Biochemistry*, vol. 52, no. 37, pp. 6335–6347, 2013, doi: 10.1021/bi400705n.

[25] T. M.Cairns *et al.*, "Surface Plasmon Resonance Reveals Direct Binding of Herpes Simplex Virus Glycoproteins gH/gL to gD and Locates a gH/gL Binding Site on gD," *J. Virol.*, vol. 93, no. 15, pp. 1–21, 2019, doi: 10.1128/jvi.00289-19.

[26] E.Engvall andP.Perlmann, "Enzyme-linked immunosorbent assay (ELISA) quantitative assay of immunoglobulin G," *Immunochemistry*, vol. 8, no. 9, pp. 871–874, 1971, doi: 10.1016/0019-2791(71)90454-X.

[27] T.Seiyama, A.Kato, K.Fujiishi, andM.Nagatani, "A New Detector for Gaseous Components Using Semiconductive Thin Films," *Anal. Chem.*, vol. 34, no. 11, pp. 1502–1503, 1962, doi: 10.1021/ac60191a001.

[28] D. R.Thévenot, K.Toth, R. A.Durst, andG. S.Wilson, "Electrochemical biosensors: Recommended definitions and classification," *Biosens. Bioelectron.*, vol. 16, no. 1–2, pp. 121–131, 2001, doi: 10.1016/S0956-5663(01)00115-4.

[29] K.Dill, D. D.Montgomery, A. L.Ghindilis, K. R.Schwarzkopf, S. R.Ragsdale, andA.V.Oleinikov, "Immunoassays based on

electrochemical detection using microelectrode arrays," *Biosens. Bioelectron.*, vol. 20, no. 4, pp. 736–742, 2004, doi: 10.1016/j.bios.2004.06.049.

[30] P.Geoffroy, M.Legrand, C.Hermann, andB.Fritig, "High-performance liquid chromatography of proteins : Purification of plant enzymes by ion-exchange chromatography," *J. Chromatogr.*, vol. 315, pp. 333–340, 1984. Available: https://doi.org/10.1016/S0021-9673(01)90750-2.

[31] A. F.Gavela, D. G.García, J. C.Ramirez, andL. M.Lechuga, "Last Advances in Silicon-Based Optical Biosensors," *Sensors*, vol. 16, pp. 1–15, 2016, doi: 10.3390/s16030285.

[32] M. S.Luchansky andR. C.Bailey, "High-Q optical sensors for chemical and biological analysis," *Anal. Chem.*, vol. 84, no. 2, pp. 793–821, 2012, doi: 10.1021/ac2029024.

[33] E.Luan, H.Shoman, D. M.Ratner, K. C.Cheung, andL.Chrostowski, "Silicon photonic biosensors using label-free detection," *Sensors*, vol. 18, no. 10, pp. 1–42, 2018, doi: 10.3390/s18103519.

[34] A. L.Washburn, L. C.Gunn, andR. C.Bailey, "Label-free quantitation of a cancer biomarker in complex media using silicon photonic microring resonators," *Anal. Chem.*, vol. 81, no. 22, pp. 9499–9506, 2009, doi: 10.1021/ac902006p.

[35] M. S.McClellan, L. L.Domier, andR. C.Bailey, "Label-free virus detection using silicon photonic microring resonators," *Biosens. Bioelectron.*, vol. 31, no. 1, pp. 388–392, 2012, doi: 10.1016/j.bios.2011.10.056.

[36] K. W.Kim, J.Song, J. S.Kee, Q.Liu, G. Q.Lo, andM. K.Park, "Label-free biosensor based on an electrical tracing-assisted silicon microring resonator with a low-cost broadband source," *Biosens. Bioelectron.*, vol. 46, pp. 15–21, 2013, doi: 10.1016/j.bios.2013.02.002.

[37] F.Ghasemi *et al.*, "Multiplexed detection of lectins using integrated glycan-coated microring resonators," *Biosens. Bioelectron.*, vol. 80, pp. 682–690, 2016, doi: 10.1016/j.bios.2016.01.051.

[38] M.Iqbal *et al.*, "Label-free biosensor arrays based on silicon ring resonators and high-speed optical scanning instrumentation," *IEEE J. Sel. Top. Quantum Electron.*, vol. 16, no. 3, pp. 654–661, 2010, doi: 10.1109/JSTQE.2009.2032510.

[39] S. T.Fard *et al.*, "Performance of ultra-thin SOI-based resonators for sensing applications," *Opt. Express*, vol. 22, no. 12, p. 14166, 2014, doi: 10.1364/oe.22.014166.

[40] Z.Ruan *et al.*, "Releasing the light field in subwavelength grating slot microring resonators for athermal and sensing applications," *Nanoscale*, vol. 12, no. 29, pp. 15620–15630, 2020, doi: 10.1039/d0nr00833h.

[41] C. Y.Zhao, L.Zhang, andC. M.Zhang, "Compact SOI optimized slot microring coupled phase-shifted Bragg grating resonator for sensing," *Opt. Commun.*, vol. 414, no. January, pp. 212–216, 2018, doi: 10.1016/j.optcom.2018.01.010.

[42] T.Claes, J. G.Molera, K.DeVos, E.Schacht, R.Baets, andP.Bienstman, "Label-free biosensing with a slot-waveguide-based ring resonator in silicon on insulator," *IEEE Photonics J.*, vol. 1, no. 3, pp. 197–204, 2009, doi: 10.1109/JPHOT.2009.2031596.

[43] N. L.Kazanskiy, S. N.Khonina, andM. A.Butt, "Subwavelength Grating Double Slot Waveguide Racetrack Ring Resonator for Refractive Index Sensing Application," *Sensors*, vol. 20, no. 12, p. 3416, Jun.2020, doi: 10.3390/s20123416.

[44] J.Flueckiger *et al.*, "Sub-wavelength grating for enhanced ring resonator biosensor," *Opt. Express*, vol. 24, no. 14, p. 15672, 2016, doi: 10.1364/oe.24.015672.

[45] L.Huang *et al.*, "Improving the detection limit for on-chip photonic sensors based on subwavelength grating racetrack resonators," *Opt. Express*, vol. 25, no. 9, p. 10527, 2017, doi: 10.1364/oe.25.010527.

[46] J. G.Wangüemert-Pérez *et al.*, "Subwavelength structures for silicon photonics biosensing," *Opt. Laser Technol.*, vol. 109, pp. 437–448, 2019, doi: 10.1016/j.optlastec.2018.07.071.

[47] R.Halir *et al.*, "Subwavelength-Grating Metamaterial Structures for Silicon Photonic Devices," *Proc. IEEE*, vol. 106, no. 12, pp. 2144–2157, 2018, doi: 10.1109/JPROC.2018.2851614.

[48] P.Azuelos *et al.*, "Optimization of porous silicon waveguide design for micro-ring resonator sensing applications," *J. Opt.*, vol. 20, no. 8, 2018, doi: 10.1088/2040-8986/aad01b.

[49] G. A.Rodriguez, S.Hu, andS. M.Weiss, "Porous silicon ring resonator for compact, high sensitivity biosensing applications," *Opt. Express*, vol. 23, no. 6, p. 7111, 2015, doi: 10.1364/oe.23.007111.

[50] P.Girault *et al.*, "Porous silicon micro-resonator implemented by standard photolithography process for sensing application," *Opt. Mater.*, vol. 72, pp. 596–601, 2017, doi: 10.1016/j.optmat.2017.07.005.

[51] P.Cheben, D.-X.Xu, S.Janz, andA.Densmore, "Subwavelength waveguide grating for mode conversion and light coupling in integrated optics," *Opt. Express*, vol. 14, no. 11, p. 4695, 2006, doi: 10.1364/oe.14.004695.

[52] P. J.Bock *et al.*, "Subwavelength grating periodic structures in silicon-on-insulator: a new type of microphotonic waveguide," *Opt. Express*, vol. 18, no. 19, p. 20251, 2010, doi: 10.1364/oe.18.020251.

[53] J.Gonzalo Wangüemert-Pérez *et al.*, "Evanescent field waveguide sensing with subwavelength grating structures in silicon-on-insulator," *Opt. Lett.*, vol. 39, no. 15, p. 4442, Aug.2014, doi: 10.1364/OL.39.004442.

[54] P.Cheben *et al.*, "Refractive index engineering with subwavelength gratings for efficient microphotonic couplers and planar waveguide multiplexers," *Opt. Lett.*, vol. 35, no. 15, p. 2526, 2010, doi: 10.1364/ol.35.002526.

[55] M.Odeh, K.Twayana, K.Sloyan, J. E.Villegas, S.Chandran, andM. S.Dahlem, "Mode Sensitivity Analysis of Subwavelength Grating Slot Waveguides," *IEEE Photonics J.*, vol. 11, no. 5, pp. 1–10, Oct.2019, doi: 10.1109/JPHOT.2019.2939088.

[56] X.Xu, Z.Pan, C. J.Chung, C. W.Chang, H.Yan, andR. T.Chen, "Subwavelength Grating Metamaterial Racetrack Resonator for Sensing and Modulation," *IEEE J. Sel. Top. Quantum Electron.*, vol. 25, no. 3, pp. 1–8, 2019, doi: 10.1109/JSTQE.2019.2915980.

[57] D.Erickson andD.Li, "Integrated microfluidic devices," *Anal. Chim. Acta*, vol. 507, no. 1, pp. 11–26, 2004, doi: 10.1016/j.aca.2003.09.019.

[58] Z.Wang *et al.*, "Microfluidic channels with ultralow-loss waveguide crossings for various chip-integrated photonic sensors," *Opt. Lett.*, vol. 40, no. 7, p. 1563, 2015, doi: 10.1364/ol.40.001563.

[59] M. A.Unger, H. P.Chou, T.Thorsen, A.Scherer, andS. R.Quake, "Monolithic microfabricated valves and pumps by multilayer soft lithography," *Science*, vol. 288, no. 5463, pp. 113–116, 2000, doi: 10.1126/science.288.5463.113.

Varun Soni is a graduate student in mechanical engineering with focus on advanced manufacturing and design at the University of Texas at Austin. He did his bachelor's of technology in mechanical engineering from Delhi Technological University in 2016. He worked with Suzuki as a Mechanical Engineer from 2016 to 2018. His current research interests include system design, machine learning in manufacturing and biosensing.

Ching-Wen Chang received B.S. and Ph.D. in the physics from National Sun Yat-Sen University, Taiwan, in 2009 and 2017. She got the 2-years Dragon Gate project (2016-2018) from MOST to support her Si-based EM wave biosensor research in UT Austin, US. She also obtained summer program visiting project from Interchange Association (Japan) and Ministry of Science and Technology (Taiwan) to support her solar cells research in Chiba University, in 2012. Currently, she is working in Academia Sinica, Taiwan from 2019. Her current research interests include the characterization of III–nitride semiconductor devices, molecular beam epitaxy technique, nanotechnology, silicon photonics and biosensing.

Xiaochuan Xu received the B.S. and M.S. degrees in electrical engineering from the Harbin Institute of Technology, Harbin, China, in 2006 and 2009, respectively, and the Ph.D. degree in electrical and computer engineering from the University of Texas, Austin, TX, USA, in 2013. He is currently a professor in State Key Laboratory on Tunable Laser Technology, Harbin Institute of Technology, Shenzhen, China. He has authored and

coauthored more than 100 peer-reviewed journal and conference papers and holds three U.S. patents. He also served as principle investigators of multiple small business innovation research (SBIR) and small business technology transfer research (STTR) programs supported by Air Force, NASA, DoE, and NIH. His current research interests include flexible photonics, nonlinear optics, fiber optics, and silicon photonics. He is a senior member of IEEE, and a member of OSA and SPIE.

Chao Wang is working toward the Ph.D. degree with Beijing University of Posts and Telecommunications since 2015. Currently, he is working a 2-years research project (2018-2020) from China Scholarship Council to support his biosensor research in UT Austin, US. His research interests include the characterization of silicon photonics, optical integration and bio-sensing.

Hai Yan received B.S. in optical information science and technology from Huazhong University of Science and Technology, Wuhan, China, in 2010, and M.S. in electronic engineering from Tsinghua University, Beijing, China, in 2013, and Ph.D. in electrical and computer engineering from the University of Texas at Austin, in 2017. His research interests include silicon photonics, nonlinear optics, integrated photonic biosensors, and silicon organic hybrid nanophotonic devices.

Michael D'Agati is a current PhD student in Electrical Engineering at the University of Pennsylvania under Dr. Troy Olsson. Currently, Michael is investigating wireless power transfer at long distances for use in implantable devices. He received his Bachelors of Engineering (B.E.) degree from Stony Brook University in 2018 where he worked on all-carbon scaffolds for tissue engineering using graphene and carbon nanotubes, and all-carbon electrodes in non-toxic supercapacitors for implantable energy storage applications, for which he won the prestigious Goldwater Scholarship in 2016.

Li-Wei Tu received his B.S. in physics from National Tsing-Hua University, Hsinchu, Taiwan and Ph.D. degree in experimental condensed matters physics from Northwestern University, Illinois, USA in 1989. He then worked at the AT&T Bell Labs, Murray Hill, New Jersey until 1995. He is currently a distinguished professor at Department of Physics, National Sun Yat-Sen University, Kaohsiung, Taiwan and works on nitride semiconductor materials and their applications. He is a Fellow of the SPIE.

Quark Yungsung Chen received his Ph.D. in 1987 from Stanford University, Palo Alto, MS in 1982 from University of Minnesota, Minneapolis and BS in 1977 from National Tsing-Hua University, Hsinchu, all in Materials Science. His doctorate work was on photoemissive small metal particles, a subject that later evolved into one of the focused research areas on plasmonics and nanotechnology. He worked at Honeywell Research Center, Minneapolis from 1987-1992 on various aspects of sensor technology and joined the Physics Department and Texas Center for Superconductivity at University of Houston in 1992 where his work was on the application of superconducting levitation and physics of oxide superconducting thin films. From 2006-2009, he was a Visiting Professor at National Sun Yat-Sen University, Kaohsiung, Taiwan where he joined its faculty in 2009 and started a research group seeking quantum structural materials, especially of oxides, nitrides and chalcogenides.

Huiping Tian received the Ph.D. degree in electrical engineering from Shanxi University, Taiyuan, China 2003 and did her 2-years Post-doctor research in Fudan University, Shanghai, China, during 2003-2005. She joined Beijing University of Posts and Communications since 2005, and currently is a distinguished professor of State Key Laboratory of Information Photonics and Optical Communications, Beijing University of Posts and Telecommunications. Her research interests include fiber communication, photonics integration and optic sensing. She is a member of OSA and IEEE.

Ray T. Chen received the B.S. degree in physics from National Tsing Hua University, Hsinchu City, Taiwan, in 1980, the M.S. degree in physics, and the Ph.D. degree in electrical engineering, from the University of California, Oakland, CA, USA, in 1983 and 1988, respectively. He holds the Keys and Joan Curry/Cullen Trust Endowed Chair at The University of Texas (UT) at Austin, Austin, TX, USA. He is the Director of the Nanophotonics and Optical Interconnects Research Lab, the Microelectronics Research Center, The UT at Austin. He is also the Director of the newly formed AFOSR MURI-Center for Silicon Nanomembrane involving faculty from Stanford, UIUC, Rutgers, and UT Austin. He joined UT Austin in 1992 to start the optical interconnect research program. From 1988 to 1992, he was a Research Scientist, Manager, and the Director of the Department of Electro-Optic Engineering, Physical Optics Corporation in Torrance, CA, USA. He was the Chief Technical Officer (CTO), Founder, and Chairman of the Board of Radiant Research, Inc. from 2000 to 2001, where he raised 18 million dollars A-Round funding to commercialize polymer-based photonic devices involving more than 20 patents, which were acquired by Finisar in 2002, a publicly traded company in the Silicon Valley (NASDAQ: FNSR). He also was the Founder and Chairman of the Board of Omega Optics Inc. since its initiation in 2001. Omega Optics has received more than five million dollars in research funding. His research work has been awarded more than 120 research grants and contracts from such sponsors as Army, Navy, Air Force, DARPA, MDA, NSA, NSF, DOE, EPA, NIH, NASA, the State of Texas, and private industry. During his undergraduate years at the National Tsing Hua University, he led the 1979 university debate team to the Championship of the Taiwan College-Cup Debate Contest. He has supervised and graduated 53 Ph.D. students from his research group at UT Austin. The research topics are focused on three main subjects: first, Nanophotonic passive and active devices for sensing and interconnect applications, second, thin film guided-wave optical interconnection and packaging for 2-D and 3-D laser beam routing and steering, and third, true time delay wideband phased array antenna (PAA). Experiences garnered through these programs in polymeric and semiconducting material processing and device integration are pivotal elements for his research work. His group at UT Austin has reported its research findings in more than 980 published papers, including more than 100 invited papers. He holds 75 issued patents. He has chaired or been a program-committee

member for more than 120 domestic and international conferences organized by IEEE, The International Society of Optical Engineering, OSA, and PSC. He has served as an Editor, Co-Editor, or coauthor for more than 20 books. He has also served as a Consultant for various federal agencies and private companies and delivered numerous invited talks to professional societies. He received the 1987 UC Regent's Dissertation Fellowship and the 1999 UT Engineering Foundation Faculty Award, for his contributions in research, teaching and services. He also received the honorary citizen award from Austin city council in 2003 for his community service contribution to black community, the 2008 IEEE Teaching Award, and the 2010 IEEE HKN Loudest Professor Award, 2013 NASA Certified Technical Achievement Award for contribution on moon surveillance conformable PAA. He is a Fellow of the OSA and SPIE.